

# Augmented-reality–guided insertion of sliding hip screw guidewire: a preclinical investigation

Carl Laverdière, MD  
 Jason Corban, MD  
 Susan Ge, MD,  
 Yukyung Kang, MD  
 Edward Harvey, MD  
 Paul A. Martineau, MD  
 Geoffroy Noel, PhD  
 Rudolf Reindl, MD

Presented at the Canadian Conference for the Advancement of Surgical Education, Oct. 29–30, 2020, the Canadian Orthopaedic Association annual meeting, June 19–20, 2020, the Jo Miller McGill Orthopaedic Visiting Professor day, June 4, 2020, Montréal, Que., and the McGill University Injury Repair Recovery Program Research Day, Feb. 27, 2020, Montréal, Que.

Accepted May 25, 2021

## Correspondence to:

C. Laverdière  
 Department of Orthopedic Surgery  
 McGill University Health Centre  
 Montreal General Hospital  
 Room A5-175.1, 1650 Cedar Ave,  
 Montréal QC H3G 1A4  
 carl.laverdiere@mail.mcgill.ca

**Cite as:** *Can J Surg* 2022 May 25; 65(3).  
 doi: 10.1503/cjs.025620

**Background:** The sliding hip screw (SHS) is frequently used in the management of hip fractures; successful placement depends on accurate positioning of the lag screw in the femoral head guided by fluoroscopy. We proposed to leverage the capabilities of augmented reality (AR) to overlay virtual images of the desired guidewire trajectory directly onto the surgical field to guide the surgeon during SHS guidewire insertion.

**Methods:** Using a commercially available AR headset and software, we performed preprocedural planning using computed tomography scans to identify the optimal trajectory for SHS guidewire insertion in the neck of a Sawbones femur model. The images of the scanned femurs containing the virtual guidewire trajectory were overlaid on the physical models such that the user could see a composite view of the computer-generated images and the physical environment. Two second-year orthopedic residents each inserted 15 guidewires under AR guidance and 15 guidewires under fluoroscopy.

**Results:** Of the 30 guidewires inserted under AR guidance, 24 (80%) were within the femoral neck, and 16 (53%) were fully enclosed within the femoral head. Nine (56%) of the 16 perforations were due to insertions that were too far along the planned trajectory. Thirteen (81%) of the successful attempts with AR had an appropriate position, compared to 25/26 (96%) with fluoroscopy. It took significantly less time to perform the procedure using fluoroscopy than AR ( $p < 0.05$ ). Fluoroscopy required on average 18.7 shots.

**Conclusion:** Augmented reality provides an opportunity to aid in guidewire insertion in a preplanned trajectory with less radiation exposure in a sterile environment, but technical challenges remain to be solved to enable widespread adoption.

**Contexte :** La vis de hanche à compression coulissante (VHCC) est souvent utilisée pour la prise en charge des fractures de la hanche; son bon positionnement dépend de l'installation précise de la vis tire-fond dans la tête fémorale sous fluoroscopie. Nous avons proposé d'utiliser les capacités de la réalité augmentée (RA) pour surimposer des images virtuelles de la trajectoire du fil-guide désirée directement sur le site opératoire dans le but de faciliter la tâche du chirurgien pendant l'insertion du fil-guide de la VHCC.

**Méthodes :** À l'aide d'un logiciel et d'un casque de RA du commerce, nous avons préplanifié l'intervention à l'aide de clichés de tomographie assistée par ordinateur (TDM) pour l'insertion optimale du fil-guide de VHCC dans le col fémoral d'un modèle de fémur Sawbones. Des clichés de TDM de fémurs montrant la trajectoire du fil guide virtuel ont été surimposés aux modèles physiques pour que l'utilisateur puisse avoir une image composite des vues générées par ordinateur et de l'environnement physique. Deux résidents de deuxième année en orthopédie ont chacun inséré 15 fils-guides à l'aide de la RA et 15 fils-guides sous fluoroscopie.

**Résultats :** Des 30 fils-guides insérés à l'aide de la RA, 24 (80 %) se trouvaient dans le col fémoral et 16 (53 %) étaient entièrement à l'intérieur de la tête fémorale. Neuf (56 %) des 16 perforations étaient dues à des insertions trop profondes le long de la trajectoire planifiée. Treize (81 %) des tentatives réussies avec la RA étaient bien positionnées, contre 25/26 (96 %) avec la fluoroscopie. L'intervention sous fluoroscopie a nécessité significativement moins de temps que l'intervention sous RA ( $p < 0,05$ ). La fluoroscopie a demandé en moyenne 18,7 clichés.

**Conclusion :** La RA offre la possibilité de faciliter l'insertion du fil-guide quand la trajectoire est préplanifiée, tout en réduisant l'exposition aux radiations dans un environnement stérile, mais il reste des difficultés techniques à régler avant de pouvoir en généraliser l'adoption.

About 1.6 million hip fractures occur annually worldwide.<sup>1,2</sup> The sliding hip screw (SHS) is an implant designed for the treatment of fractures of the proximal femur. Proper implant placement involves a cannulated lag screw inserted into the head of the femur with the assistance of a guidewire. This screw then slides within a barrel attached to a plate secured on the lateral aspect of the femur.<sup>3</sup> Owing to the limitations of current fluoroscopic imaging modalities, multiple views are frequently required to help the surgeon extrapolate 3-dimensional (3D) anatomy from 2-dimensional (2D) fluoroscopic images, with the focus of the surgeon shifting constantly between the screen and the patient.<sup>4</sup> The need to use fluoroscopy while simultaneously ensuring the correct position of the aiming guide can result in increased surgical time, surgeon fatigue, and greater radiation exposure for both patient and surgical staff, as well as the creation of multiple passes through the femoral head and neck in bone that often is already osteoporotic.

Placement of the SHS is evaluated objectively by means of the tip-to-apex distance (TAD), the sum of the distance from the tip of the screw to the apex of the femoral head on anteroposterior and lateral radiographs.<sup>5</sup> A TAD of 25 mm or less is associated with a lower rate of screw cut-out and fixation failure.<sup>5</sup> Appropriate placement of the SHS guidewire is key to ensuring that the lag screw has an appropriate TAD. Therefore, a tool that can provide direct overlay of the optimal guidewire trajectory onto the patient could minimize the guesswork of guidewire insertion and facilitate this key step in SHS fixation.

Augmented reality (AR) devices allow for the overlaying of virtual images on the user's field of view to create a composite of virtual images and real surroundings. Recently, commercially available AR devices, such as Microsoft's HoloLens, have been used to superimpose important anatomic structures directly onto the operative field.<sup>6</sup> In addition, software is being developed to allow for the overlay of holographic 3D computed tomography (CT) scans onto patient surface anatomy by means of AR devices to allow for clinical use. With these advances, we proposed that a commercially available AR device could be used to provide guidance for multiple orthopedic procedures that require guidewire insertion, including SHS insertion. Insertion of an SHS is a relatively simple procedure with a validated objective score to evaluate optimal screw position (TAD) and can be used as a proxy for the feasibility of AR-guided guidewire insertion in orthopedic procedures.

As technologic advances in orthopedic surgery allow for more minimally invasive procedures, there is a trend toward increased intraoperative radiation exposure, a potential health hazard for those who are exposed to it over the course of their career.<sup>7,8</sup> An AR approach might decrease radiation exposure, contribute to improved screw placement, simplify complex cases, and allow better assess-

ment of fracture configuration and patient anatomy, all without taking the surgeon's attention away from the operative field.<sup>9-11</sup> In addition, AR technology allows voice commands and hand motion control, permitting use under sterile conditions.

In this preclinical investigation, we used a commercially available AR headset and software to overlay CT scans, with preplanned SHS guidewire trajectories, onto phantom models of proximal femurs. We hypothesized that screws can be placed inside a bone more accurately with the proposed AR system than with the use of fluoroscopy.

## METHODS

This investigation was performed at the McGill University Health Centre, Montréal. The study was approved by the McGill University Faculty of Medicine Institutional Review Board (#A03-M11-19B).

### Outcomes

The TAD was the primary outcome. The goal was to replicate an SHS insertion with a TAD less than 25 mm.<sup>5</sup> Time for insertion, deviation of the guidewire from the preplanned entry point and exit point, any perforation of the guidewire out of the femur models through the femoral head or the femoral neck at any point, and number of fluoroscopy shots (and associated dosage, in milligray) required were secondary outcomes.

### Femur model

We created femur models by encasing an anatomic femur replica (Sawbones #1130) in a radiolucent LePage Tite polyurethane foam. The femurs were aligned anatomically and encased such that no part of the bone was visible from the outside.

### Augmented reality

The AR headset used in this experiment was the Microsoft HoloLens 1. This device, which uses combiner lenses and a holographic processor unit, produces virtual images by projecting 2 sets of beams, creating a sculptural casting of the light waves on real objects and thus generating interactive holograms with respect to the user's real environment.<sup>12</sup> The user can interact with the headset by voice command or hand gestures in front of the device.

We downloaded the Novarad OpenSight AR image application onto the AR headset and used it to integrate the CT data with AR. This software works by rebundling the CT DICOM images into a proprietary file format, allowing full integration of the images as 1 complete 3D volume. This complete volume rendering is then projected through the AR headset to allow the user to visualize the CT data as

a recreated 3D hologram. The software includes interface modes to allow the cross-sectional images of the 3D volume to be viewed in axial, coronal, sagittal and oblique views. The window level can also be adjusted, allowing different densities of material or tissue to be visualized according to the Hounsfield scale.

*Preprocedural planning*

We performed a CT scan of the femur models before guidewire insertion with a Philipps Brilliance iCT Family CT machine. The models were scanned with a slice thickness of 0.67 mm, with an increment of 0.67 mm to ensure sufficient image detail.

We processed the DICOM images using the Novarad picture archiving and communication system software, annotating the images with a virtual needle that would produce a perfectly placed SHS with a TAD of 0. The virtual needle consisted of 2 circles (1 at the entry point in the bone and 1 at the end point at the femoral head) and a red line going through the circles and projecting outside the model (Figure 1). This information was then saved on the CT scan and exported into the AR image application. This allowed for visualization of the needle trajectories overlaid onto the physical models via the AR headset.

*Guidewire placement*

Two second-year orthopedic residents (J.C., S.G.) each inserted 15 SHS guidewires under AR guidance and 15 guidewires under fluoroscopy (control). The preprocedural plan (CT scan with planned screw trajectories) was opened in the AR headset by means of the associated AR image application to allow for visualization of DICOM images and trajectories in hologram mode. The user

aligned the hologram to the model manually, using hand gestures to transpose and rotate the hologram, and to adjust the window as needed until alignment was determined to be satisfactory at all angles. The AR image software has an element called a spatial anchor that is used to maintain the spatial accuracy of the hologram while the user moves throughout the room. Once the physical and virtual models were aligned, the underlying Sawbones femur, trajectory guide, and planned entry and end point were visible over the model. The software enabled toggling between views of the outer shell of the model, the inner section of the model and the individual 2D slices (axial, coronal and sagittal), which could be scrolled through by means of hand motion.

The residents then placed the guidewire-free hand on the foam to match the entry point, making sure the wire was within the bull’s eye of the circular entry point of the virtual needle and parallel to the planned trajectory (Figure 2). They then drove the guidewire into the model with a drill. At the point where the K-wire entered bone, they measured the planned distance of the screw from the foam to the centre of the femoral head using a caliper and marked it on the wire. Once this mark touched the edge of the foam, the wire was not driven in any farther.

In both the AR and the control group, anteroposterior and lateral fluoroscopic images were obtained after the procedure to evaluate the position of the K-wire and to calculate the TAD. The time required for insertion and number of fluoroscopy shots required were also recorded.

*Assessment of guidewire placement*

We calculated the TAD for all insertions using fluoroscopy. We used the anteroposterior and lateral views to

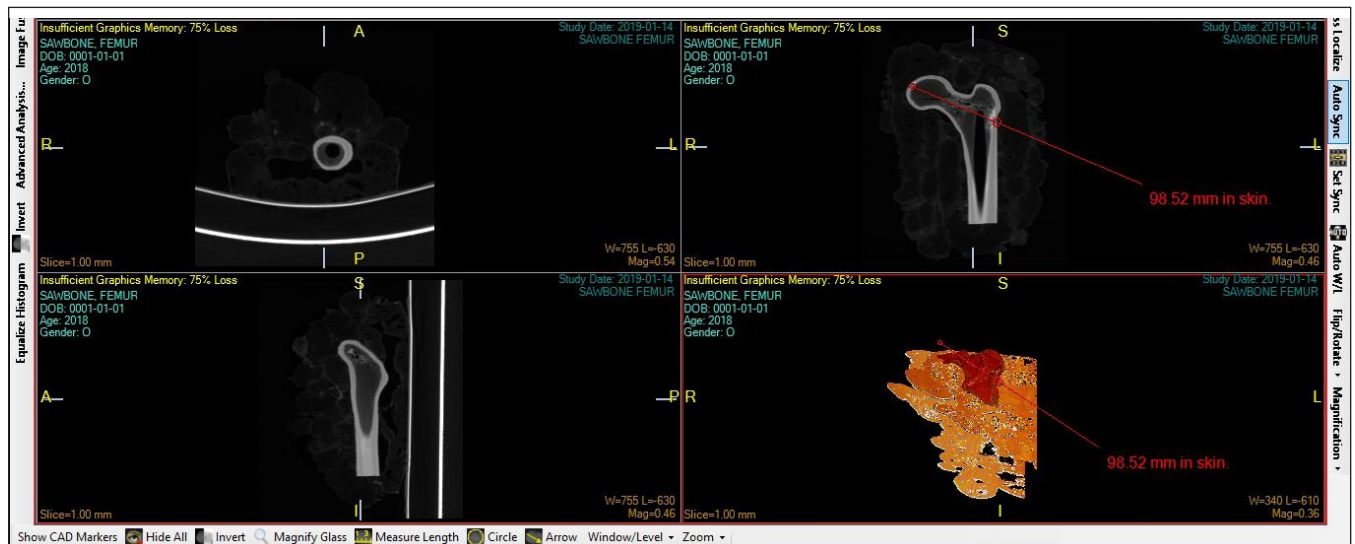
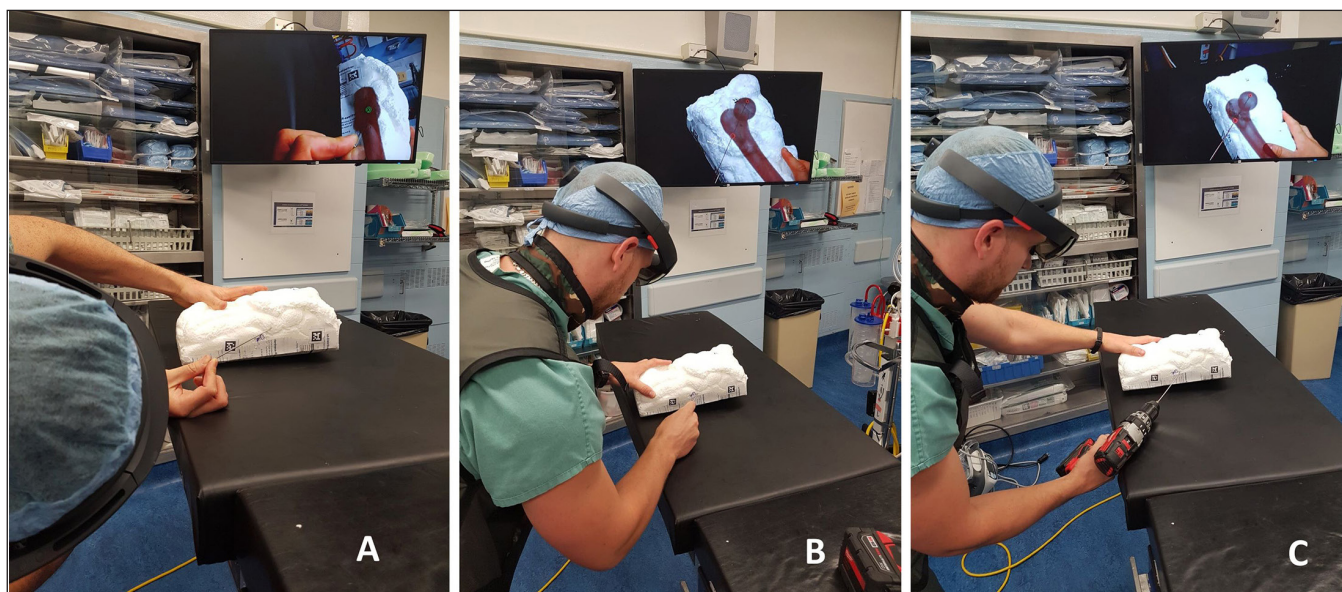
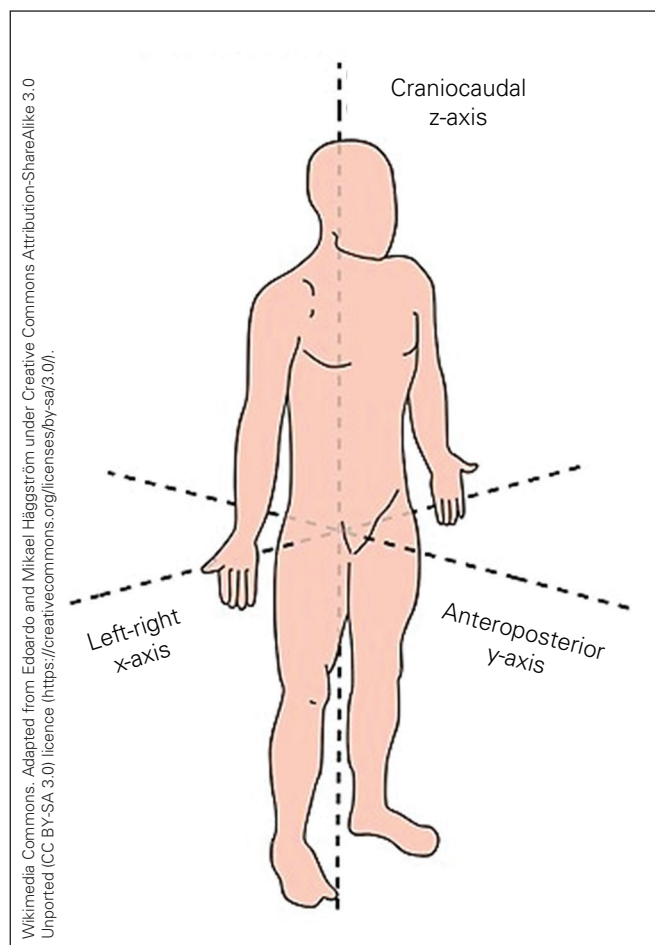


Fig. 1. Preprocedural planning of needle insertion using the Novarad OpenSight DICOM planning software.





**Fig. 2.** Insertion procedure. (A) The K-wire was inserted while making sure it followed the planned trajectory. When it was in the bull's eye position, the 2 circles became green. (B) The user made sure the K-wire followed the trajectory in the anteroposterior plane. (C) Once the K-wire was properly placed, it was loaded on a drill and inserted to the proper depth. To show what the user was seeing, a television screen was equipped with a Microsoft wireless display adaptor plugged in the HDMI port, which allowed for screen mirroring from the HoloLens to the screen.



**Fig. 3.** Reference axes for spatial orientation of the guidewire.

visualize the location of the guidewire relative to the bone. We also measured the amount of deviation of the guidewire from the preplanned entry point and exit point, and any perforation of the guidewire at any point out of the femur model through the femoral head or the femoral neck.

To quantify the location of the guidewires, we used a spatial orientation system with the axes defined as shown in Figure 3. Left, anterior and caudal were considered positive values.

### Statistical analysis

We used basic descriptive analysis and a paired Student *t* test (with  $p = 0.05$  deemed statistically significant) for comparative data. All statistical analysis was conducted with the MATLAB software suite (MATLAB R2018a, MathWorks).

## RESULTS

### Tip-to-apex distance

The success rate was 87% (26/30) with fluoroscopy and 53% (16/30) with AR. The TAD was less than 25 mm for 13 (81%) of the 16 successful insertions with AR and 25 (96%) of the 26 successful insertions with fluoroscopy. The mean TAD for the successful insertions by resident 1 using AR was 21.47 mm (standard deviation [SD] 4.67 mm) versus 21.00 mm (SD 7.07 mm) with fluoroscopy (Table 1), a nonsignificant difference

( $p = 0.6$ ). The mean TAD for the successful insertions by resident 2 using AR was 16.36 mm (SD 7.38 mm) versus 12.16 mm (SD 9.48 mm) with fluoroscopy ( $p = 0.03$ ).

With the unsuccessful attempts, the mean TAD per perforation under AR guidance was 19.52 mm (SD 7.24 mm) for resident 1 and 29.20 mm (SD 15.67 mm) for resident 2.

**Accuracy of entry and exit points with augmented reality**

The mean error for resident 1 was 14.34 mm (SD 7.85 mm) at the entry point of the guidewire and 12.01 mm (SD 6.70 mm) at the end point (Table 1, Figure 4 and Figure 5). At the entry point, the mean error was 8.48 mm (SD 8.78 mm [range -4.01 mm to 22.39 mm],  $p = 0.005$ ) on the y-axis and 5.03 mm (SD 10.05 mm [range -25.32 mm to 12.89 mm],  $p = 0.1$ ) on the z-axis. At the end point, the mean error was -2.74 mm (SD 5.21 mm [range -12.45 mm

to 9.48 mm],  $p = 0.2$ ) on the x-axis, 3.95 mm (SD 12.15 mm [range -14.75 mm to 26.29 mm],  $p = 0.3$ ) on the y-axis and 1.54 mm (SD 6.68 mm [range -7.41 mm to 12.60 mm],  $p = 0.6$ ) on the z-axis.

For resident 2, the mean error was 12.00 mm (SD 6.63 mm) at the entry point and 12.16 mm (SD 9.48 mm) at the end point. At the entry point, the mean error was 9.11 mm (SD 6.84 mm [range -1.63 mm to 23.21 mm],  $p = 0.005$ ) on the y-axis and 1.82 mm (SD 8.01 mm [range -16.23 mm to 11.56 mm],  $p = 0.5$ ) on the z-axis. At the end point, the mean error was -3.12 mm (SD 6.95 mm [range -18.24 mm to 4.71 mm],  $p = 0.2$ ) on the x-axis, -3.08 mm (SD 13.40 mm [range -26.29 mm to 19.31 mm],  $p = 0.5$ ) on the y-axis and 2.28 mm (SD 11.34 mm [range -23.20 mm to 11.69 mm],  $p = 0.5$ ) on the z-axis.

There was no statistically significant difference between the 2 users in mean error at the entry point ( $p = 0.8$  and  $p =$

**Table 1. Results for resident 1 and resident 2 with augmented reality and fluoroscopy**

Resident no.	Order of insertion	Augmented reality						Fluoroscopy (control)				
		Within femoral head	Within femoral neck	Total time, min:s	TAD, mm	Mean error entry point, mm	Mean error tip, mm	Time total, min:s	TAD, mm	Total no. of radiographs	Time, s	Cumulative dosage, mGy
1	1	Yes	Yes	4:43	27.75	16.73	27.95	1:39	21.17	14	17.4	0.25
	2	No	Yes	7:29	-24.80	12.96	17.69	2:18	21.21	15	14.2	0.22
	3	No	Yes	5:22	-28.82	25.06	23.73	6:12	34.61	39	36.2	0.57
	4	Yes	Yes	5:16	12.39	11.53	11.06	4:20	18.5	32	33.1	0.47
	5	Yes	Yes	5:30	21.37	11.28	3.68	2:23	34.12	21	20.7	0.32
	6	Yes	Yes	4:20	22.10	4.09	8.00	2:17	22.25	17	16.3	0.27
	7	Yes	Yes	2:33	23.98	4.13	12.47	1:29	28.78	7	17.3	0.27
	8	Yes	No	2:30	50.72	13.28	7.79	3:10	17.43	23	28.0	0.42
	9	Yes	Yes	5:13	24.65	12.53	14.80	3:12	25.04	11	25.8	0.23
	10	Yes	No	4:05	16.64	20.37	8.61	1:28	19.69	11	26.0	0.23
	11	No	Yes	8:00	-14.70	9.88	10.13	3:01	11.09	24	29.0	0.44
	12	Yes	Yes	6:12	19.76	31.75	8.86	2:03	16.73	12	19.2	0.32
	13	Yes	Yes	5:30	24.52	3.88	6.03	5:07	17.32	27	49.2	0.75
	14	No	Yes	6:15	-18.11	18.34	12.97	1:34	12.19	15	19.3	0.30
	15	No	Yes	5:45	-11.15	19.31	6.37	2:15	14.89	12	19.4	0.31
Mean	—	—	—	5:15	22.76	14.34	12.01	2:50	21.00	18.6	24.4	0.36
2	1	No	No	7:46	-31.76	17.96	20.87	3:35	20.87	20	32.60	0.55
	2	Yes	Yes	3:17	11.88	24.15	4.65	1:07	4.65	16	17.60	0.28
	3	No	No	3:17	-57.70	3.42	11.60	2:17	11.60	28	28.90	0.43
	4	No	Yes	3:20	-26.76	7.58	15.58	1:30	15.58	17	23.50	0.40
	5	No	Yes	2:35	-8.94	21.25	1.44	1:16	1.44	11	11.60	0.18
	6	Yes	Yes	3:17	10.06	12.51	2.07	1:11	2.07	12	16.20	0.27
	7	No	Yes	3:57	-15.22	15.03	1.96	2:28	1.96	30	28.40	0.44
	8	No	Yes	6:31	-47.05	3.90	31.48	1:01	31.48	13	18.50	0.29
	9	No	No	2:37	-34.02	17.56	24.49	5:09	24.49	42	47.00	0.70
	10	No	Yes	2:29	-15.88	9.81	4.62	1:23	4.62	15	17.70	0.28
	11	No	Yes	3:23	-25.48	1.97	22.34	1:28	22.34	15	20.50	0.33
	12	Yes	Yes	2:46	20.94	16.93	18.32	1:02	18.32	11	15.20	0.26
	13	Yes	Yes	5:29	11.06	7.82	5.57	2:20	5.58	19	14.20	0.15
	14	Yes	Yes	4:51	29.08	11.82	7.55	2:32	7.56	20	32.40	0.54
	15	Yes	No	12:42	15.14	11.29	9.87	1:14	9.88	13	9.00	0.10
Mean	—	—	—	4:33	24.06	12.20	12.16	1:58	12.16	18.8	21.49	0.33

TAD = tip-to-apex distance.

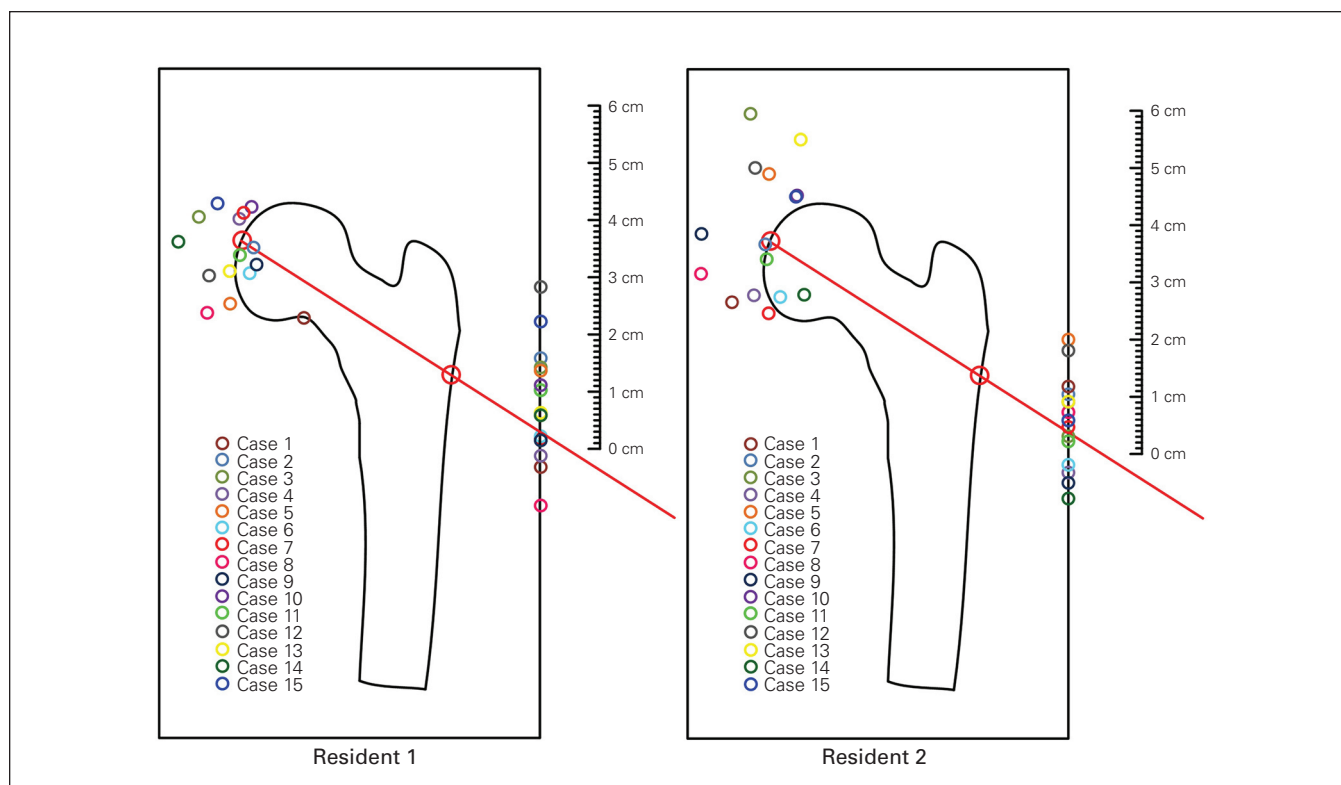


**Fig. 4.** Scaled schematic showing the error distribution of the 2 residents using the augmented reality system in the anteroposterior view.



**Fig. 5.** Scaled schematic showing lateral view of the insertion for the 2 residents. The circles represent the entry point, and the squares represent the tip/end point.

0.3 for the y-axis and z-axis, respectively) or the end point ( $p = 0.9$ ,  $p = 0.1$  and  $p = 0.3$  for the x-axis, y-axis and z-axis, respectively).

Of the 30 K-wires, 24 (80%) were completely within the femoral neck; 13 (54%) of the 24 were also fully enclosed in the femoral head. Nine (56%) of the 16 perforations through the femoral head were due to insertion of the guidewire too far along the planned trajectory. Two wires (7%) were within the femoral head but not in the femoral neck.

#### *Procedure time and radiation exposure*

On average, it took 3 minutes for resident 1 to align the model and 2 minutes 14 seconds to insert the K-wire using AR; the corresponding times for resident 2 were 2 minutes 24 seconds and 2 minutes. For both users, it took significantly less time to perform guidewire insertion using fluoroscopy (mean 2 min 50 s and 1 min 58 s for residents 1 and 2, respectively) than using AR (mean 5 min 15 s and 4 min 33 s for residents 1 and 2, respectively) ( $p < 0.05$ ).

Fluoroscopy required on average 18.6 radiograph shots and exposure to 0.36 mGy per insertion for resident 1, and 18.8 radiograph shots and exposure to 0.33 mGy per insertion for resident 2.

## DISCUSSION

In our investigation, fluoroscopic SHS guidewire insertion was more accurate than AR-guided insertion. Although 80% of wires were within the femoral neck with AR, the rate of successful insertion in the femoral neck without perforation through the femoral head was 43%, compared to 100% with fluoroscopy. In the successful attempts where the K-wire trajectory was through the femoral neck and head without perforation, the mean TAD for resident 1 was 21.47 mm (SD 4.67 mm) with AR and 21.00 mm (SD 7.07 mm) with fluoroscopy, both within the acceptable range of less than 25 mm, with no significant difference between the 2 methods. Although there was a significant difference between AR and fluoroscopy ( $p = 0.03$ ) for resident 2, that user achieved a lower mean TAD for successful insertions than resident 1 with both AR (16.36 mm [SD 7.38 mm]) and fluoroscopy (12.16 mm [SD 9.48 mm]). The results suggest that, when the guidewire did not perforate the femoral head, the TAD with AR-guided insertion appeared comparable to that with fluoroscopy.

On initial comparison, the accuracy obtained with AR in our investigation seems lower than that in a previous investigation in which the software combination was used to place spinal needles as a proxy for pedicle screws.<sup>9</sup> However, Gibby and colleagues<sup>9</sup> extrapolated their pedicle screw trajectory based on entry point, without actually inserting a screw. Further interpretation of our data shows that the majority of unsuccessful attempts were due to perforation through the femoral head. This may have been due to error in manual alignment of the virtual and physical femur models, or lack of tip tracking.

At the time of our investigation, the software required that the holograms be aligned to the physical models manually, which may have affected accuracy and prolonged total procedure time. Furthermore, although the program is designed such that the virtual holograms remain stable in space once aligned, a small amount of movement was noticed when the user moved to different angles, which necessitated further microadjustments. In addition, the holograms were not sufficiently transparent to see through to the physical models, which made it difficult to align the virtual and physical models without adjusting the contrast and to visualize the entry point of the physical guidewire past the holographic projection of the planned trajectory. All these factors were likely a source of decreased accuracy, which is reflected in the magnitude of the mean error in the entry points, 14.34 mm (SD 7.85 mm) for resident 1 and 12.00 mm (SD 6.63 mm) for resident 2. In a real oper-

ative scenario, this would make it difficult to see anatomic landmarks during the procedure. These challenges regarding manual overlay and hologram micromotion were not discussed by Gibby and colleagues,<sup>9</sup> who reported an accuracy of 97% maximal deviation radius of 2.5 mm when placing spinal needles at the entry point to mimic the trajectory of pedicle screws. We speculate that, if the issues regarding automatic overlay are rectified, results will be greatly improved.

The users compensated for the lack of tip-tracking ability by inserting guidewires to a depth measured off the planned trajectory from the tip of the femur to the most lateral aspect of the femoral shaft. This measure was determined crudely with a caliper and a marking pen, which was used to indicate the depth at which the wire should be stopped. Since the planned end point was the apex of the femoral head, an entry point that differed from what was initially planned could ultimately lead to a propagation of error and perforation. In addition, because the planned end point was at the tip of the femoral head, any error would easily have resulted in insertion past the tip. If we had stopped slightly short of the measured distance or had planned to be more in the subchondral area instead of right at the tip, we likely would have obtained much better results.

Guidewire insertion in Sawbones models does not give the same tactile feedback as insertion in real bone, which makes perforation out of the bone more difficult to assess. Gibby and colleagues<sup>9</sup> assessed potential deviation in the mediolateral and craniocaudal planes but did not evaluate the depth of needle placement, as no needle was advanced into bone; thus, we cannot directly compare our results regarding perforation. Improved technology for surface mapping and tip tracking would make AR technology more usable in the clinical setting and would likely result in improved accuracy in reproducing planned K-wire trajectories.

The mean procedure time with AR was nearly double that with fluoroscopy for both residents. This difference was likely secondary to challenges with manually overlaying the holograms over the models, which took about 55% of the total procedure time, and to the steeper learning curve associated with AR.

## Limitations

Most patients undergoing SHS insertion would not have a CT scan of their hip available for conversion into a hologram. However, we chose SHS guidewire insertion as a validation model as it is relatively simple procedure with a quantitative parameter for clinical success. We hope that this model can be used as an initial method not only for assessing accuracy, but also for determining limitations of AR in more complex procedures for which patients would have preoperative CT scans, such as sacroiliac screw placement. Another avenue of further investigation is the use of



fluoroscopic images with AR, which some centres have already started to explore.<sup>13,14</sup> There are currently fluoroscopic machines that can provide low-radiation CT scans as well, which could potentially allow AR to be used even in simple procedures like dynamic hip screw insertion in the future.

Some technical issues regarding the ergonomics of the HoloLens should be highlighted. Although the device weighs only 579 g, both users reported that it was front-heavy. When coupled with the potential for eye fatigue as well as motion sickness,<sup>15-17</sup> there is an obvious ergonomic barrier to prolonged use. Other challenges encountered included issues regarding poor fit on certain facial structures, and the potential for background movement and noise to interfere with functions. These issues should be rectified with newer iterations of the HoloLens and other AR headsets.

## CONCLUSION

Our results suggest that commercially available AR devices have the capacity for obtaining accurate results in the placement of SHS guidewires while diminishing exposure to radiation. However, modifications need to be made with respect to accurate surface mapping and tip tracking to improve precision and to avoid harmful complications, such as femoral perforation. Despite evidence suggesting that the initial use of an AR headset may result in increased operative time, automated hologram positioning and increased exposure to AR may help rectify this in future iterations of AR hardware and software.

**Affiliations:** From the Department of Orthopedic Surgery, McGill University Health Centre, Montreal General Hospital, Montréal, Que. (Laverdière, Corban, Ge, Kang, Harvey, Martineau, Reindl); and the Department of Anatomy and Cell Biology, McGill University, Montréal, Que. (Noel).

**Competing interests:** Edward Harvey reports grants or contracts from the Canadian Institutes of Health Research (CIHR), the US Department of Defense and the Natural Sciences and Engineering Research Council of Canada. He holds dozens of patents for orthopedic devices and methods outside the submitted work. He has participated on a CIHR institute advisory board, and has played a leadership role for the Orthopaedic Trauma Association. He holds stock in MY01 and NXTSENS Microsystems. He is also coeditor-in-chief of *C7S*; he was not involved in the review of this manuscript nor in the decision to accept it for publication. No other competing interests were declared.

**Contributors:** C. Laverdière, J. Corban, S. Ge, P. Martineau and R. Reindl designed the study. Y. Kang and G. Noel acquired the data, which E. Harvey analyzed. C. Laverdière, J. Corban, S. Ge and Y. Kang wrote the manuscript, which E. Harvey, P. Martineau, G. Noel and R. Reindl critically revised. All authors gave final approval of the article to be published.

**Content licence:** This is an Open Access article distributed in accordance with the terms of the Creative Commons Attribution (CC BY-

NC-ND 4.0) licence, which permits use, distribution and reproduction in any medium, provided that the original publication is properly cited, the use is noncommercial (i.e., research or educational use), and no modifications or adaptations are made. See: <https://creativecommons.org/licenses/by-nc-nd/4.0/>.

## References

- Cooper C, Campion G, Melton LJ 3rd. Hip fractures in the elderly: a world-wide projection. *Osteoporos Int* 1992;2:285-9.
- Gullberg B, Johnell O, Kanis JA. World-wide projections for hip fracture. *Osteoporos Int* 1997;7:407-13.
- Chirodian N, Arch B, Parker MJ. Sliding hip screw fixation of trochanteric hip fractures: outcome of 1024 procedures. *Injury* 2005;36:793-800.
- Mentis HM, Chellali A, Manser K, et al. A systematic review of the effect of distraction on surgeon performance: directions for operating room policy and surgical training. *Surg Endosc* 2016;30: 1713-24.
- Baumgaertner MR, Solberg BD. Awareness of tip-apex distance reduces failure of fixation of trochanteric fractures of the hip. *J Bone Joint Surg Br* 1997;79:969-71.
- Pratt P, Ives M, Lawton G, et al. Through the HoloLens™ looking glass: augmented reality for extremity reconstruction surgery using 3D vascular models with perforating vessels. *Eur Radiol Exp* 2018;2:2.
- Mastrangelo G, Fedeli U, Fadda E, et al. Increased cancer risk among surgeons in an orthopaedic hospital. *Occup Med (Lond)* 2005; 55:498-500.
- Singer G. Occupational radiation exposure to the surgeon. *J Am Acad Orthop Surg* 2005;13:69-76.
- Gibby JT, Swenson SA, Cvetko S, et al. Head-mounted display augmented reality to guide pedicle screw placement utilizing computed tomography. *Int J Comput Assist Radiol Surg* 2019;14:525-35.
- Laverdière C, Corban J, Khoury J, et al. Augmented reality in orthopaedics: a systematic review and a window on future possibilities. *Bone Joint J* 2019;101-B:1479-88.
- Wang H, Wang F, Leong APY, et al. Precision insertion of percutaneous sacroiliac screws using a novel augmented reality-based navigation system: a pilot study. *Int Orthop* 2016;40:1941-7.
- Chaudhari A, Lakhani K, Deulkar K. Transforming the world using holograms. *Int J Comput Appl* 2015;130:30-2.
- Unberath M, Fotouhi J, Hajek J, et al. Augmented reality-based feedback for technician-in-the-loop C-arm repositioning. *Healthc Technol Lett* 2018;5:143-7.
- von der Heide AM, Fallavollita P, Wang L, et al. Camera-augmented mobile C-arm (CamC): a feasibility study of augmented reality imaging in the operating room. *Int J Med Robot* 2018;14.
- Hanna MG, Ahmed I, Nine J, et al. Augmented reality technology using Microsoft HoloLens in anatomic pathology. *Arch Pathol Lab Med* 2018;142:638-44.
- Mahmood F, Mahmood E, Dorfman RG, et al. Augmented reality and ultrasound education: initial experience. *J Cardiothorac Vasc Anesth* 2018;32:1363-7.
- Tepper OM, Rudy HL, Lefkowitz A, et al. Mixed reality with HoloLens: where virtual reality meets augmented reality in the operating room. *Plast Reconstr Surg* 2017;140:1066-70.